

# Curcumin: A Multipurpose Matrix for MALDI Mass Spectrometry Imaging Applications

S. Francese,<sup>\*,†</sup> R. Bradshaw,<sup>†</sup> B. Flinders,<sup>†</sup> C. Mitchell,<sup>†</sup> S. Bleay,<sup>‡</sup> L. Cicero,<sup>†</sup> and M. R. Clench<sup>†</sup>

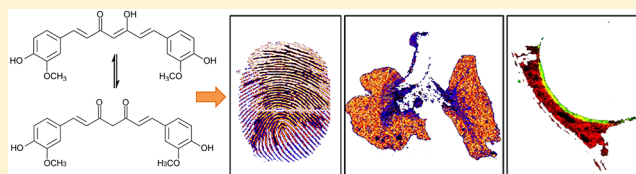
<sup>†</sup>Sheffield Hallam University, Biomedical Research Centre, Howard Street, S1 2GT Sheffield, United Kingdom

<sup>‡</sup>Home Office, Centre for Applied Science and Technology, Sandridge, AL4 9HQ ST Albans, United Kingdom

## S Supporting Information

**ABSTRACT:** Curcumin, 1,7-bis-(4-hydroxy-3-methoxy-phenyl)-hepta-1,6-diene-3,5-dione, is a polyphenolic compound naturally present in the *Curcuma longa* plant, also known as turmeric. Used primarily as a coloring agent and additive in food, curcumin has also long been used for its therapeutic properties in a number of medical scenarios. Here, we report on an entirely novel use of curcumin; its extended structure of

conjugated double bonds suggested the potential of this compound to be a good matrix assisted laser desorption ionization mass spectrometry (MALDI MS) matrix candidate. In the quest for novel and more efficient MALDI MS matrices, curcumin is revealed to be a versatile and multipurpose matrix. It has been applied successfully for the analysis of pharmaceuticals and drugs, for imaging lipids in skin and lung tissues, and for the analysis of a number of compound classes in fingermarks. In each case, the use of curcumin is shown to promote analyte ionization very efficiently as well as provide excellent mass spectral image quality.



**T**urmeric (*Curcuma longa*) is a rhizomatous herbaceous plant belonging to the ginger family Zingiberaceae. The main components of turmeric are 1,7-bis-(4-hydroxy-3-methoxy-phenyl)-hepta-1,6-diene-3,5-dione (also known as curcumin), which can exist in keto and enol forms (tautomers), and its desmethoxy and bis-desmethoxy derivatives which are present in varying ratios (Figure 1).

Curcumin is commonly employed in the Indian subcontinent where it has 2000 years of history and tradition for use in food preservation and coloring, in medicine, and as a fabric dye.<sup>1</sup> Most interesting is the biological and medical properties documented for this compound. It is extensively used in Ayurvedic medicine for its antioxidant,<sup>2,3</sup> anti-inflammatory,<sup>4</sup> analgesic, and antiseptic properties.<sup>5,6</sup> Curcumin has been shown to have the potential to act as a therapeutic agent for a variety of severe medical conditions, including liver disorders, diabetes, cardiovascular and Alzheimer's disease, HIV, and different types of cancer, with discoveries supported by extensive peer-reviewed literature and ongoing clinical trials.<sup>7–9</sup>

The antiviral, immunosuppressant, chemopreventive, and chemotherapeutic properties<sup>7–9</sup> of curcumin are due to its ability to intervene in multiple signaling pathways, as Hatcher and colleagues report in their review.<sup>10</sup> The remarkable variety of beneficial properties has gained curcumin the nickname of "Spice for Life".

In 2011, Garg and collaborators<sup>11</sup> reported on another possible application for curcumin; this time in the context of forensic science. Exploiting its golden color property, this compound was used in its original source as turmeric powder to dust latent fingermarks on different surfaces. Garg and co-workers demonstrated strong enhancement of fingermarks on a number of both porous and nonporous surfaces justifying the

adherence to the latent fingermarks as a result of hydrogen bond formation between the fatty acids/glycerides of sebum contained in the mark and the carbonyl and hydroxyl group of the curcumin. Good contrast was achieved, especially on darker surfaces, with the added advantage of turmeric being nontoxic in contrast to other conventional powders used in fingerprint dusting techniques.

The possibility of using turmeric as a latent fingerprint enhancer and the observation that curcumin exhibits a highly conjugated double bond structure may suggest the possibility to employ turmeric/curcumin as a dual agent for both fingerprint visualization and as an effective matrix in the chemical imaging of fingerprints by matrix assisted laser desorption ionization mass spectrometry (MALDI MS). Francese's group has previously reported on the 2 step dry-wet method of matrix application whereby alpha cyano-4 hydroxycinnamic acid was employed as dual agent to: (i) provide a fingerprint image, useful for suspect identification, captured in a conventional forensic fashion thus enabling evidence to be presented in a Court of Law and (ii) gather chemical information, via MALDI MSI, potentially crucial in providing important investigative leads.<sup>12</sup> Concerning point (i), natural curcumin has fluorescent properties in the visible green spectrum<sup>13</sup> and this feature could further help with the visualization and the image capture of latent marks.

Although curcumin has been characterized both qualitatively and quantitatively by laser desorption ionization (LDI) and MALDI MS,<sup>14,15</sup> it was never suggested that this compound

Received: March 11, 2013

Accepted: April 26, 2013

Published: April 26, 2013

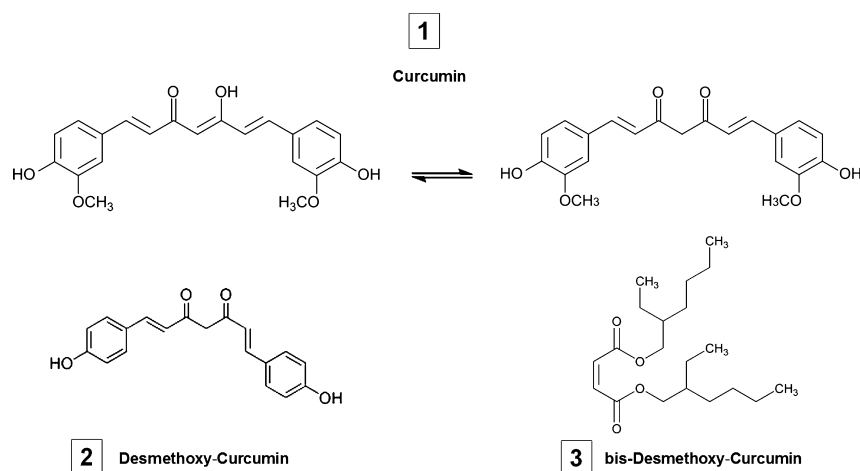


**Figure 1.** Main components of tumeric powder: Curcumin, 1,7-bis-(4-hydroxy-3-methoxy-phenyl)-hepta-1,6-diene-3,5-dione ( $C_{21}H_{20}O_6$ , monoisotopic MW 368.1258) existing in a tautomeric form, and its desmethoxy ( $C_{20}H_{18}O_5$ , monoisotopic MW 338.1154) and bis-desmethoxy ( $C_{19}H_{16}O_4$ , monoisotopic MW 308.1048) derivatives.

could act as a MALDI matrix itself. Here, we report on the use of curcumin in such capacity as well as showing versatility of this matrix for a number of different analytes (drugs, lipids, peptides, and proteins), imaging applications, and different biological specimens including fingermarks, lung tissues, and skin.

## EXPERIMENTAL SECTION

**Materials.** Curcumin from *curcuma longa* (Turmeric) powder, polyethylene glycol (PEG),  $\alpha$ -cyano-4-hydroxycinnamic acid ( $\alpha$ -CHCA), trifluoroacetic acid (TFA), analytical grade methanol, Acitretin, carboxymethylcellulose (CMC), and ALUGRAM1 SIL G/UV254 precoated aluminum sheets were obtained from Sigma-Aldrich (Poole, UK). Acetone, acetonitrile (ACN), and glass microscope slides were purchased from Fisher Scientific (Loughborough, Leicestershire, UK). Tiotropium bromide was kindly provided by GlaxoSmithKline (Stevenage, UK). MALDI target OPTI TOF spotless inserts were purchased from Applied Biosystems (Foster City, CA, USA). Double-sided conductive carbon tape was purchased from TAAB (Aldermaston, UK). Dulbecco's phosphate-buffered saline and Dulbecco's modification of Eagle's medium, used for tissue washing and MTT incubations of living skin equivalents, were purchased from Invitrogen (Paisley, UK).

**Instrumentation.** All mass spectrometric analyses were conducted on either a modified Applied Biosystems API Q-Star Pulsar i hybrid quadrupole time-of-flight (QTOF) instrument (Concord, Ontario, Canada) or a Waters MALDI HDMS Synapt G2 mass spectrometer (Waters Corporation, Manchester, UK) equipped with an Nd:YAG laser operated at 1 kHz. In the Q-Star instrument, the orthogonal MALDI source has been modified to incorporate a SPOT 10 kHz Nd:YVO<sub>4</sub> solid-state laser (Elforlight Ltd., Daventry, UK),<sup>16</sup> having a wavelength of 355 nm and a pulse duration of 1.5 ns and producing an elliptical spot size of 100  $\mu$ m  $\times$  150  $\mu$ m.

**Methods. Tissue Samples. Lung Tissues.** Lung tissues were sourced from Brown Norway rats and were a kind donation by GSK. All animal studies were ethically reviewed and carried out in accordance with Animals (Scientific Procedures) Act 1986 and the GSK Policy on the Care, Welfare and Treatment of Laboratory Animals.

**Skin Tissues.** All living skin equivalent (LSE) samples were provided by Evocutis as "LabSkin" in collaboration with Stiefel, a GSK company. The LSE batches were delivered as inserts within transport culture medium and were carefully handled in an ethical manner. The LSE units were partially suspended in Dulbecco's modification of Eagle's medium so that the cells were continually nourished.

**Sample Preparation. Synthesis of Curcumin.** Synthetic curcumin was synthesized according to the method reported by Pabon.<sup>17,18</sup>

**Standards Preparation.** Tiotropium bromide was prepared from a 1 mg/mL stock solution in methanol adjusted to free base, to give a 100 ng/ $\mu$ L standard in 50% methanol. Acitretin was prepared from a 1 mg/mL stock solution in a 4:1 acetone/olive oil vehicle. The solution was further diluted (from the use of the vehicle only solution) to give a 0.2% acitretin working solution. Cocaine (0.1 mg/mL) and paracetamol (1 mg/mL) were prepared in 50:50 methanol/H<sub>2</sub>O solution. A mixture of bovine insulin ( $m/z$  5735), cytochrome C ( $m/z$  12361), and apomyoglobin ( $m/z$  16952) was prepared at a concentration of 0.5  $\mu$ g/ $\mu$ L in 70:30 acetonitrile/water.

**Specimen Preparation.** (a) **Fingerprint Preparation:** Ungroomed latent fingerprints were prepared as described previously<sup>19</sup> pressing the fingertips upon the desired surface with a pressure between 40 and 50 g (0.39–1.49 N). In another set of experiments, ungroomed fingerprints were divided either into two halves or into quarters. An ungroomed fingerprint was also deposited on an Aluminum sheet to be subjected to MALDI MS analysis of peptides and small proteins. Cocaine contaminated fingerprints were prepared by dipping an ungroomed fingertip into a 1 mg/mL methanolic cocaine solution. The fingers were then rubbed together to ensure an even distribution of cocaine on the fingertips before depositing a mark onto a ceramic tile. Fingertips were immediately washed with 70:30 methanol/water wipes.

(b) **Lung Tissue Preparation:** Frozen control Brown Norway rat lung tissue was sectioned using a Leica CM3050 cryostat (Leica Microsystems, Wetzlar, Germany) to produce 10  $\mu$ m thick sections, which were thaw mounted onto glass slides.

(c) **Skin Preparation:** Aliquots (100  $\mu$ L) of Acitretin (0.2%) dissolved in the 4:1 acetone/olive oil solution vehicle were topically administered onto the LSE samples. These treated

samples were incubated in 5% CO<sub>2</sub>, 37 °C for 4 h. At the end of the incubation period, excess treatment on the surface was carefully washed off with Dulbecco's phosphate-buffered saline. To quench metabolism, samples were snap-frozen within liquid-nitrogen cooled isopentane and stored at -80 °C prior to analysis. Skin tissue sections (12 μm) were cut using a cryostat (Leica 2000 UV, Leica Microsystems, Milton Keynes, UK) and thaw-mounted onto conventional glass slides. The mounted sections were washed with deionized water to remove any excess salts and other impurities from the skin.

**Matrix Application. Profiling Experiments.** Tiotropium, cocaine, and paracetamol standards were individually mixed (1:1) with 2 mg/mL in 70:30 acetonitrile/0.5% TFAaq curcumin solution; 1 μL of each mixture was spotted onto a MALDI target plate. 0.2% of the acitretin standard was mixed (1:1) with a 2 mg/mL in 70:30 acetonitrile/0.2% TFAaq curcumin solution, and 1 μL of the mixture was spotted also onto a MALDI target plate. Peptide/protein mixed standards were mixed 1:1 with a solution of 2 mg/mL curcumin in either 70:30 ACN/H<sub>2</sub>O or 70:30 ACN/0.5%TFAaq. An ungroomed fingermark was spotted with a solution of 2 mg/mL curcumin in 70:30 ACN/H<sub>2</sub>O for peptide/protein analysis.

**Imaging Experiments: Lung Imaging.** For the initial experiments, 20 mL of a 10 mg/mL solution of commercial curcumin in 70:30 acetonitrile/0.2% TFAaq was applied onto a control rat lung tissue section using the Iwata Eclipse HP-CS gravity feed airgun (Iwata-Media Inc., Portland, USA). In another experiment, a 2 mg/mL solution of synthetic curcumin in 70:30 acetone/0.5% TFAaq was spotted using the Labcyte Portrait 630 reagent multispotter (Labcyte, California, USA) using 10 cycles with 100 μm spot-to-spot distance. In a final set of experiments, acetone was successfully replaced by acetonitrile; a 2 mg/mL solution of synthetic curcumin in either 70:30 ACN/0.5% TFAaq or 70:30 ACN/H<sub>2</sub>O was applied onto consecutive control rat lung tissue sections by the Labcyte Portrait 630 using the same settings as above.

**Skin Sample Preparation.** Matrices were deposited onto skin sections using a SunCollect automated sprayer. In one experiment, a 2 mg/mL synthetic curcumin in a 70:30 ACN/0.2% TFAaq solution was applied. In a separate experiment, one-third of the skin section was spray coated with a 2 mg/mL synthetic curcumin in a 70:30 ACN/0.2% TFAaq solution; one-third of the skin section was sprayed with 5 mg/mL  $\alpha$ -cyano-4-hydroxycinnamic acid ( $\alpha$ CHCA) and in 70:30 ACN/0.2% TFAaq, and one-third was left unsprayed. The specific regions of the tissue were covered with foil during the matrix application. Separate capillaries for the autosprayer were also used to avoid cross contamination, respectively. The SunCollect was set to deposit 5 layers of matrix using a medium raster speed rate (with the capillary tip positioned at 41 mm above the sample). In particular, the first layer was sprayed at 3.5 μL/min whereas the remaining 4 layers were sprayed at 1 μL/min.

**Fingermark Preparation.** Two ungroomed fingermarks were divided into halves and dusted using either synthetic or commercial curcumin, with excess powder being removed using a Klenair Air Duster. Either the solvent free method of matrix application<sup>20</sup> or the previously optimized dry-wet<sup>12</sup> method were subsequently employed. In a separate experiment, two fingermarks were treated using either synthetic curcumin or  $\alpha$ -CHCA via the dry-wet method. For the ungroomed fingermark split into quarters, the matrix was applied as follows: (i) curcumin via the dry-wet method; (ii) curcumin via the solvent

free method; (iii)  $\alpha$ -CHCA via the solvent free method; (iv)  $\alpha$ -CHCA via the dry-wet method. In the dry-wet method, the interested fingermark portions were sprayed using the SunCollect autosprayer with a 70:30 ACN/0.5% TFAaq solution to allow for co-crystallization of the matrix with the fingermark analyte residue. A total of 5 layers were sprayed at a rate of 5 μL/min using a "medium" raster speed. The other two quarters were left untreated. The four quarters were then placed onto the same MALDI plate in the initial orientation (to form a full fingermark) and analyzed in a single experiment by MALDI MS imaging. The same autosprayer settings were also employed in the preparation of a cocaine contaminated fingermark for MS/MS imaging experiments.

**Mass Spectrometric Analyses.** MALDI MS spectra of drugs were obtained on the Q-Star mass spectrometer in positive ion mode in the mass range between  $m/z$  50 and 1000. Declustering potential 2 was set at 15 arbitrary units, and the focus potential was 20 arbitrary units, with an accumulation time of 0.117 min. The MALDI MS/MS spectrum of the cocaine precursor ion at  $m/z$  304.15 was obtained using argon as the collision gas; the declustering potential 2 was set at 10, and the focusing potential was 30. The collision energy and the collision gas pressure were set at 20 and 12 arbitrary units, respectively. Profiling mass spectra of a mixture of peptide/proteins standard and of an ungroomed fingermark were acquired on a MALDI Voyager De-STR (Applied Biosystems) in the range of 5–17 kDa and 2–10 kDa, respectively. Positive ion spectra were acquired in linear mode using 300 shots per spectrum at 25 000 V with the grid set to 93% and extraction delay time of 150 ns. Fingermark images were acquired on the Q-Star instrument at a spatial resolution of 150 μm × 150 μm in "Raster Image" mode;<sup>21</sup> each image was acquired in around 90 min run time. Mass spectra were processed in Analyst MDS Sciex (Concord, Ontario, Canada). Skin images were also acquired on the Q-Star instrument at a spatial resolution of 50 μm × 50 μm in positive ion mode analysis within the mass range of 50–1000  $m/z$ . All images were converted using "oMALDI Server 5.1" software supplied by MDS Sciex (Concord, Ontario, Canada) and processed using Biomap (Novartis, Basel). All the images were generated using the freely available Novartis Biomap 3.7.5.5 software (Novartis, Basel, CH).

Lung images were acquired on the MALDI HDMS SYNAPT G2 mass spectrometer. Prior to MALDI-ion mobility spectrometry-mass spectrometry imaging (MALDI-IMS-MSI) analysis, the samples were optically scanned using a CanoScan 4400F flatbed scanner (Canon, Reigate, UK) to produce a digital image for future reference; this image was then imported into the MALDI imaging pattern creator software (Waters Corporation) to define the region to be imaged. The instrument was calibrated prior to analysis using a standard mixture of polyethylene glycol. The instrument was operated in sensitivity mode and positive ion mode at a spatial resolution of 100 μm × 100 μm, with ion mobility separation in the mass range of  $m/z$  100 to 1000. The data were then converted using MALDI imaging converter software (Waters Corporation) and visualized using Biomap 3.7.5.5 software. Lung images were also acquired on the Q-Star instrument at a spatial resolution of 150 μm × 150 μm in positive ion mode in the mass range of  $m/z$  100–1000 and data processed by Biomap 3.7.5.5.

**Data Processing.** Mass spectra from Analyst and from the region of interest in Biomap were converted into txt files and then imported into mMass,<sup>22</sup> an open source multifunctional

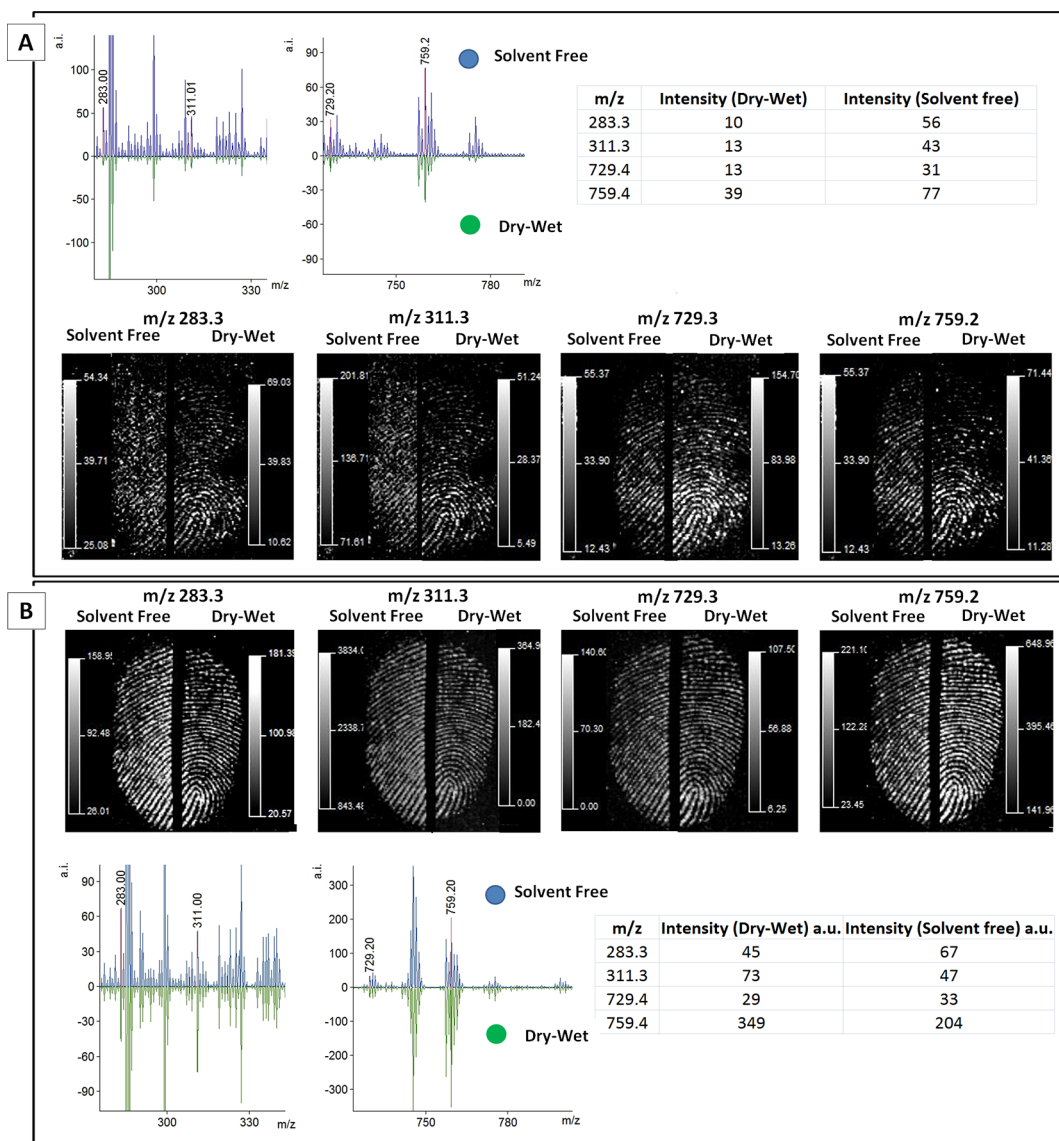


**Figure 2.** Comparative MALDI MS imaging of ungroomed fingermarks using either commercial or synthetic curcumin. MALDI images are generally more intense, and ridges are clearer when using synthetic curcumin (Panel B) instead of the commercial variety (Panel A), when applying both the solvent free and the dry-wet method. Higher signal intensity (for the four lipids selected as examples) can also be seen by comparing the spectra and the tables for each curcumin source.

mass spectrometry software. Spectra were viewed, smoothed and, in the case of small molecules, internally recalibrated using the curcumin ion signals or the  $\alpha$ -CHCA ion signals according to the experiment performed.

## RESULTS AND DISCUSSION

Following on the findings reported by Garget et al.,<sup>11</sup> that curcumin is a suitable agent to enhance fingermarks from a variety of surfaces, these authors examined its structure and hypothesized a possible role of this compound as a MALDI matrix, initially for latent fingermark analysis via the dry-wet method as previously reported.<sup>12</sup> However, prior to assessing the efficiency of curcumin as a MALDI matrix, curcumin was synthesized according to Pabon<sup>17</sup> and MALDI mass spectral profiles were obtained for both its commercial and synthetic forms. As expected, the synthetic form exhibited a lot less spectral background compared to the commercially available curcumin (Figure S1, Supporting Information), which is known

to be a mixture of curcuminoids. Both synthetic and commercial curcumin were initially employed to analyze ungroomed fingermarks (prepared as described elsewhere<sup>19</sup>) by MALDI MSI in the  $m/z$  range of 100–1000. In particular, after enhancing the mark using a Zephyr brush (Figure S2, Supporting Information), the performance of curcumin was assessed both as a solvent free matrix<sup>20</sup> and within the dry-wet method of matrix application.<sup>12</sup> On the basis of the results shown in Figure 2, an immediate observation can be made that the synthetic curcumin produces a lot clearer images of the ridge detail (Figure 2B) than the commercial one (Figure 2A) in both solvent free and dry-wet method applications. This probably could be due to a nonoptimal analyte/matrix ratio, given that curcumin is mixed with other curcuminoids in the commercial variety. Fingermark images were not normalized as, often, during the normalization process, details of the ridges can be lost (as discussed further in this paper). They were, however, adjusted to the optimum contrast/brightness giving the best clarity of the *minutiae* (local characteristics of the ridge

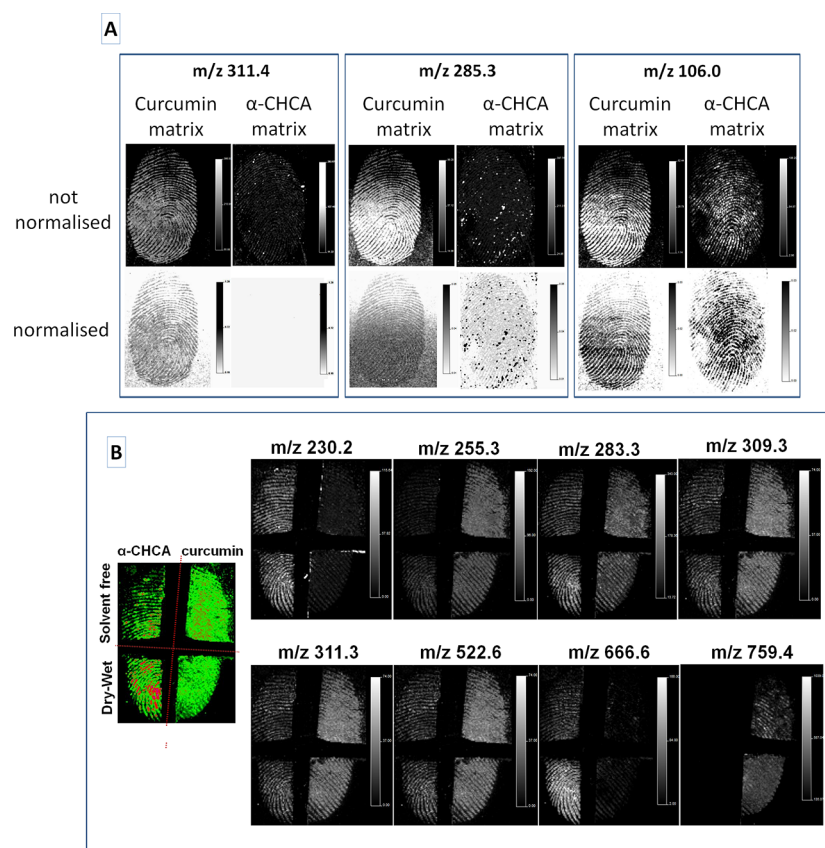


**Figure 3.** Comparative MALDI MS imaging of ungrooved fingermarks using either synthetic curcumin or  $\alpha$ -CHCA. Panel A shows molecular maps of three endogenous species imaged either by the use of curcumin or  $\alpha$ -CHCA according to the dry-wet method. Images are reported both normalized and not normalized to maximize the range of possible observations. In a separate experiment (Panel B), an ungrooved mark was split in quarters which were each treated with one of the following methods: (a) solvent free ( $\alpha$ -CHCA), (b) dry-wet method ( $\alpha$ -CHCA), (c) solvent free (curcumin), and (d) dry-wet method (curcumin). Lipid molecular maps were reported for a comparative evaluation of the four methods.

pattern). A region of interest was drawn on each fingermark area, and the corresponding peak list was exported in text format and imported into mMass. The mass spectra (obtained using both matrix types and application methods) were showed in pairs by flipping one of the spectra (Figure 2). In the case of the synthetic curcumin, the differences in intensity for two fatty acids (oleic acid at  $m/z$  283.3 and eicosenoic acid at 311.3) and two glycerophospholines (at  $m/z$  729.4 and  $m/z$  759.4), reported as examples, are not dramatic between the two methods of application used; this shows that both the solvent free and the dry-wet method successfully enable these species to ionize and be mapped. In the case of the commercial curcumin, both application methods seem to work in a similar way, with the solvent free method providing generally higher intensity peaks than the dry-wet method. This suggests that the generally unsatisfying results in this case can be ascribed solely to the nature of the commercial powder.

Synthetic curcumin performance was also assessed against the use of the matrix  $\alpha$ -CHCA (normally employed for this MALDI MSI application<sup>12,19</sup> by the use of the dry-wet method). For this purpose, two ungrooved fingermarks generated in the same instance were deposited on a ceramic tile (Figure 3). Images are displayed in Figure 3A, both as normalized (against the total ion current, TIC) and not normalized. Normalized images allow an immediate comparison of the efficiency of the two matrices in terms of ion intensity whereas non-normalized images often allow the ridges to be observed with more clarity. As it can be seen from Figure

3A, the species selected as an example at  $m/z$  311.4 (eicosenoic acid), at  $m/z$  285.3 (stearic acid), and at  $m/z$  106.0 (possible serine, reported to be the most abundant amino acid in fingermarks<sup>23</sup>) all exhibit higher image intensity when curcumin was used instead of  $\alpha$ -CHCA. Another experiment was performed by dividing the fingermark in quarters and treating them with (i) solvent free ( $\alpha$ -CHCA), (ii) dry-wet method ( $\alpha$ -CHCA), (iii) solvent free (curcumin), and (iv) dry-wet method (curcumin) to enable a more in depth comparison (Figure 3B). Results show that ionization with one or the other matrix is species dependent and that it is not possible to establish superiority of either one of the two matrices. For example, the glycerophosphocoline at  $m/z$  759.4 is ionized by curcumin but not by  $\alpha$ -CHCA. On the contrary, the diacylglycerol at  $m/z$  666.6 is better ionized by  $\alpha$ -CHCA than by curcumin. The species at  $m/z$  283.3 (oleic acid) seems to ionize equally well with both matrices. The clarity of the ridge detail in this experiment may appear to contradict the previous result in Figure 2B. However, it has to be considered that, although every effort is made to keep the contact pressure/time the same during the deposition as well as to have a similar way to brush the matrix, this may not always be consistent; therefore, clarity of the ridges may be compromised by variability of pressure/contact time in all or a specific area of the mark and across the experiments performed. Results from Figure 3B allow us to conclude that both  $\alpha$ -CHCA and curcumin are efficient matrices for lipids in fingermarks within the  $m/z$  range between 100 and 1000 and that both the solvent free and the dry-wet

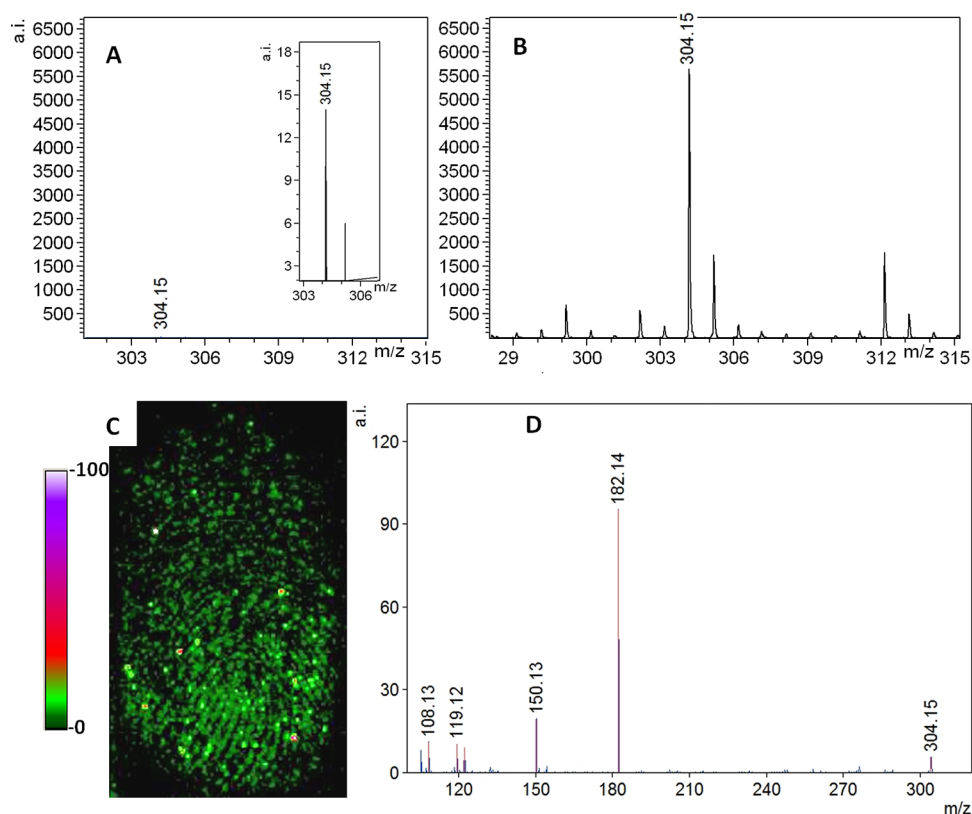


**Figure 4.** MALDI MS profiling and MS/MS imaging of cocaine. Panels A and B show the LDI and MALDI MS analysis via curcumin matrix of cocaine. Panel C shows the MALDI MS/MS image of cocaine (via its fragment at  $m/z$  182.1) in a spiked fingermark. An MS/MS spectrum was extracted from one of the pixel spots in the image showing a higher concentration of cocaine in which all the expected cocaine product ions are detected (Panel D).

method are similarly efficient. The general reason behind the success of the solvent free method could be explained by the presence of residual moisture in the fresh fingermark. It is likely that, with older marks in which the moisture has disappeared, cocrystallization with the analytes may not happen.

Finally, to further explore the feasibility of curcumin as a MALDI matrix for the analysis of fingermarks, an ungrooved mark was spiked with a cocaine solution and a MALDI MS/MS imaging experiment was performed. Prior to this, cocaine was analyzed both in LDI and in MALDI MS mode to ensure that curcumin was in fact responsible for the ionization of this compound. As expected, in LDI conditions, the sensitivity is very poor (Figure 4A) compared to that in MALDI conditions via the use of curcumin (Figure 4B). This confirms effectiveness of this matrix in assisting the ionization of small molecules such as drugs. Furthermore, cocaine could be ionized, fragmented, and mapped through its most intense signal at  $m/z$  182.1 (Figure 4C). The image has been normalized against the TIC. The MS/MS spectrum could be extracted by selecting one of the sweet spots in the image to show all the expected ion fragments for cocaine<sup>24</sup> (Figure 4D).

In order to investigate its versatility as a MALDI matrix, synthetic curcumin was also employed as a matrix for different analytes and specimens to image. Three other drugs tiotropium bromide (TB), acitretin, and paracetamol, administered in respiratory and skin diseases and as an antipyretic/analgesic, respectively, were profiled by MALDI MS along with a mixture of peptides and proteins (Figure S3, Supporting Information). Although both TB and acitretin can also be analyzed, with less efficiency, in LDI conditions, in both cases, satisfying ion signals

could be obtained at  $m/z$  392.08 ( $[M]^+$ ), (Figure S3A, Supporting Information) and at 326.19 and 327.19  $m/z$  (acitretin and protonated acitretin, respectively) (Figure S3B, Supporting Information); paracetamol, previously detected only by MALDI MSI using  $\alpha$ -CHCA,<sup>25</sup> has been detected in this work as  $(M + H)^+$  ion at  $m/z$  152.07 using curcumin as a matrix (Figure S3C, Supporting Information). Standard peptides/proteins have been detected at  $m/z$  5734 (insulin), 11 361 (cytochrome C (Cyt C)), and 16 951 (myoglobin). Insulin, Cyt C, and myoglobin ion signals could be much better detected if TFA was not added to the curcumin solution during preparation (Figure S3D,E, Supporting Information), despite curcumin being a more efficient proton donor in the presence of acid.<sup>26</sup> When curcumin is dissolved in acid, it turns from bright red to a yellow color; as Sharma et al. have reported,<sup>27</sup> in acidic conditions, within the keto form of curcumin, the heptadienone linkage between the two methoxyphenol rings contains a highly activated carbon atom. The CH carbon bonds on this carbon are very weak due to delocalization of the unpaired electron on the adjacent oxygen atoms. This curcumin formulation (no acid) was also employed to successfully detect peptides and small proteins within ungrooved fingermarks (Figure S3F, Supporting Information) reproducing the work of Ferguson et al.<sup>12</sup> who had used in their work  $\alpha$ -CHCA instead. Subsequent studies focused on the use of curcumin to image lipids and small molecules from two different specimens and of two widely used matrix depositors which were available in the laboratory, namely, the acoustic spotter (Portrait 630) and an automatic sprayer (SunCollect).

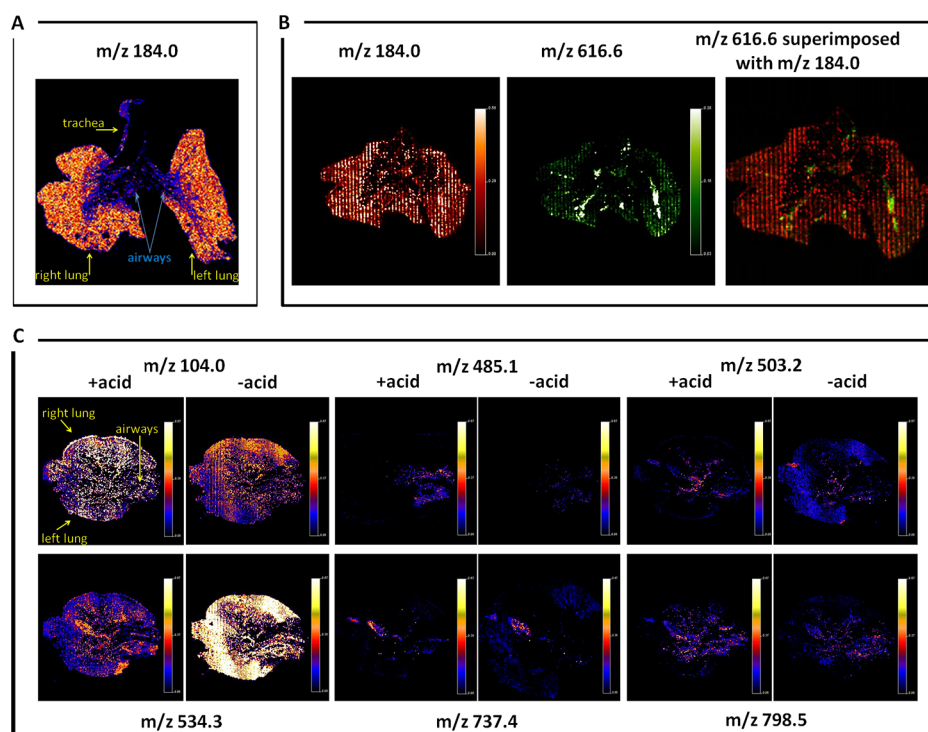


**Figure 5.** MALDI-MS images of control rat lung tissue. Panel A shows the MS image of phosphocoline at  $m/z$  184.0. The image was obtained by spray coating the section with curcumin and acquiring the data on the Synapt G2 HDMS operated in positive and sensitive mode at  $100\ \mu\text{m} \times 100\ \mu\text{m}$  spatial resolution. Panel B shows the MS images of the heme group at  $m/z$  616.6 and phosphocoline at  $m/z$  184.0 as well as their image superimposition. The images were acquired by depositing curcumin with the acoustic spotter Portrait 630, and acquisition was performed on the Q-Star instrument at  $150\ \mu\text{m} \times 150\ \mu\text{m}$  spatial resolution. Panel C shows a comparison of MALDI MS images of control rat lung tissue sections which were spotted by a curcumin solution either with or without TFA. Acquisition was performed on the Q-Star mass spectrometer at  $150\ \mu\text{m} \times 150\ \mu\text{m}$  spatial resolution. All images were normalized to the total ion count. Images were adjusted to the same brightness and contrast except those in Panels A and B.

The first specimen considered was control rat lung tissue which was manually sprayed with a solution of curcumin as described in the Methods section. The resulting images, of which Figure 5A reports an example, showed in very good detail the different anatomical regions such as the trachea and the airways. A second set of experiments was performed by spotting curcumin with the Portrait 630 acoustic spotter using acetone to dissolve curcumin. Even in this case, results were satisfying in displaying the fine structures of the rat lung tissue section, as the superimposition of the heme ion signal ( $m/z$  616.6) with the phosphocoline ion signal ( $m/z$  184.0) shows (Figure 5B). Comparative experiments were also performed whereby curcumin was deposited using the Portrait 630 acoustic spotter either with or without TFA (Figure 5C). Although, as previously discussed, the addition of acid makes curcumin a strong proton donor, significant differences in the image ion intensity were not found and the efficiency of ionization is species specific. For example, whereas choline ionizes more efficiently when acid is added to the matrix solution, the species at  $m/z$  534.3 exhibits the opposite trend.

Finally, experiments were performed using skin as a biological specimen (LSE). LSE are three-dimensional living entities, made from primary human fibroblasts and keratinocyte cells cultured in multiple layers. The resulting differentiated product has the composition and handling characteristics of human skin. Acitretin was applied to the surface of LSE specimens and allowed to penetrate for 4 h prior to wash off excess. Curcumin was subsequently spray coated prior to analysis by MALDI MSI (Figure 6A). All images were

normalized to the TIC and optimized for brightness and contrast. Curcumin allowed ionization of several classes of lipids; Figure 6A reports as an example the ion at  $m/z$  496.4, likely to be a lysophosphatidylcholine, at  $m/z$  703.6, a sphingomyelin, both signals located in the dermis (histology not shown), and at  $m/z$  718.6, possibly PC(O-14:0/18:1), distributed both in the epidermis and possibly in the hypodermis, in agreement with Hart et al.<sup>28</sup> Moreover, the nonprotonated acitretin ( $m/z$  326.2) image (exhibiting a higher intensity signal than the protonated molecule) could be superimposed with the image of phosphocoline at  $m/z$  184.0 showing penetration of the drug in the epidermis. To assess efficiency of curcumin as a matrix against the efficiency of  $\alpha$ -CHCA as well as ionization in LDI conditions, a second experiment was performed whereby a section of acitretin treated LSE was divided into three parts, with each section treated as follows; sprayed with  $\alpha$ -CHCA, left unsprayed, and sprayed with curcumin (Figure 6B). Many ion signals could be imaged, including acitretin ( $m/z$  326.2), choline ( $m/z$  104.0), and phosphocoline ( $m/z$  184.0). The ion signal of these species was stronger in the curcumin sprayed area of the skin section when compared to that sprayed with  $\alpha$ -CHCA. The presence of acitretin in the unsprayed region is in agreement with previous experiments showing that acitretin could be ionized under LDI conditions (not shown). However, its ion signal exhibits a lot higher intensity when curcumin is used indicating a role of this compound as a matrix in assisting acitretin ionization. The superimposition of the acitretin image with that of the ion at  $m/z$  758.6 (possibly glyceropholipid) shows, again, a greater

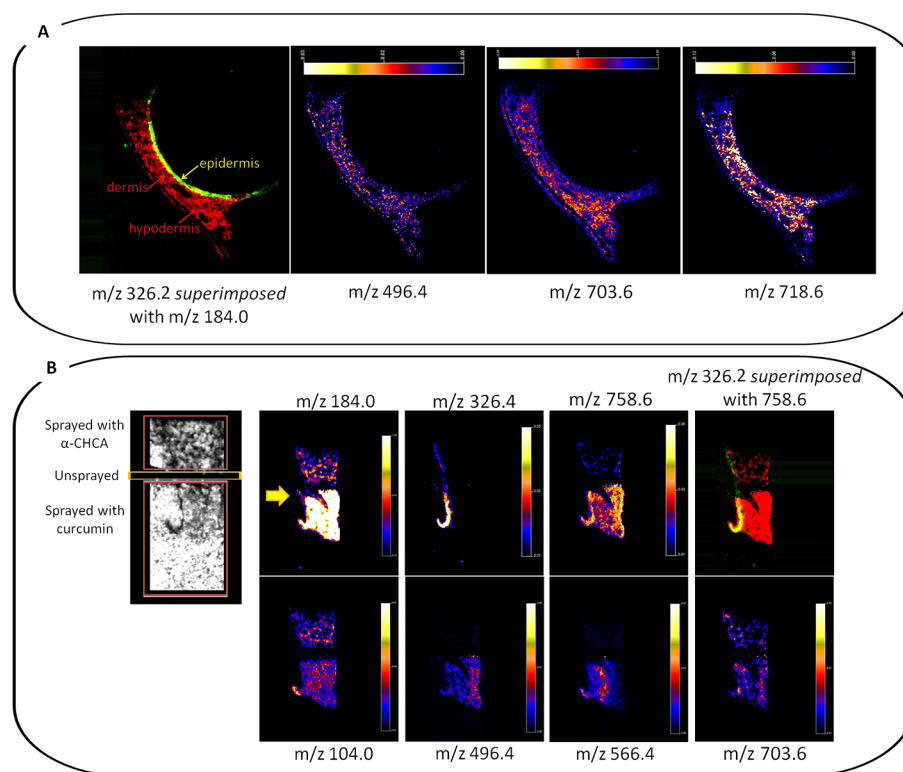


**Figure 6.** MALDI MS/MS imaging at  $50\ \mu\text{m} \times 50\ \mu\text{m}$  spatial resolution of Labskin equivalents treated with acitretin. Panel A shows MALDI images of acitretin ( $m/z\ 326.4$ ) superimposed with phosphocholine ( $m/z\ 184.0$ ) and other two lipids at  $m/z\ 703.6$  and  $718.8$ . Panel B shows a skin section treated with three regions treated in three different ways: sprayed coated with  $\alpha$ -CHCA, no matrix, and spray coated with curcumin. Several lipids were imaged which generally showed a much higher signal intensity in the curcumin sprayed region and absence of signal in the unsprayed area. Acitretin ion was reported both as a single MALDI image and superimposed with the lipid at  $m/z\ 758.6$  showing presence also in the unsprayed region but exhibiting superior ion intensity in the curcumin sprayed region. Acitretin was applied in the direction of the yellow arrows.

abundance in the distribution of both species in the curcumin sprayed area against the  $\alpha$ -CHCA sprayed area. Other lipid images were reported such as those at  $m/z\ 496.4$ , putative as lysophosphatidylcholine (displayed also in Figure 6A), and  $566.4$  (possibly monoacylglycerophosphoglycerol), both showing dominant presence in the curcumin sprayed region, whereas the ion at  $m/z\ 703.6$  (possible sphingomyelin) was present in both the  $\alpha$ -CHCA and curcumin treated regions with a slightly higher distribution in the latter region. These experiments show that curcumin is an extremely efficient matrix for different lipid classes and drug ionization in skin and, in several cases, it outperforms  $\alpha$ -CHCA.

## CONCLUSIONS

The work presented here demonstrates that curcumin can be used as a novel MALDI matrix. Very similar to  $\alpha$ -CHCA in terms of versatility, it can be employed for different classes of analytes ranging from small molecules (drugs and lipids) to possibly larger ones (peptides and small proteins) as the profiling of peptides and small proteins contained in fingerprints shows. The study also shows that it is preferable to use synthetic curcumin rather than that commercially available from Sigma Aldrich. This is clearly shown when applied to MALDI MSI of fingerprints. Curcumin has been applied in this work manually and by means of the lab available automatic spraying and acoustic spotting systems (SunCollect and Portrait 630) although the authors recommend using a dedicated capillary when using the SunCollect autospraying system. Versatility of curcumin is also demonstrated by the possibility to image a

range of different biological specimens, in addition to fingerprints, such as lung tissues and skin. Altogether, this work allows us to conclude that curcumin can be employed to enrich the armor of MALDI matrices especially for MALDI MSI applications.

## ASSOCIATED CONTENT

### Supporting Information

Additional information as noted in text. This material is available free of charge via the Internet at <http://pubs.acs.org>.

## AUTHOR INFORMATION

### Corresponding Author

\*Tel: +441142256165. Fax: +441142253066. E-mail: [s.francese@shu.ac.uk](mailto:s.francese@shu.ac.uk).

### Notes

The authors declare no competing financial interest.

## ACKNOWLEDGMENTS

Dr. Akram Khan is gratefully acknowledged for helping with the synthesis of curcumin. GSK and GSK/Stiefel are also gratefully acknowledged for funding PhD students B.F. and C.M. enabling them to contribute to the present work.

## REFERENCES

- (1) Ammon, H.; Wahl, M. A. *Planta Med.* **1991**, *57*, 1–7.
- (2) Jefremov, V.; Zilmer, M.; Zilmer, K.; Bogdanovic, N.; Karelson, E. *Ann. N.Y. Acad. Sci.* **2007**, *1095*, 449–457.



- (3) Sreejayan, N.; Rao, M. N. *J. Pharm. Pharmacol.* **1994**, *46*, 1013–1016.
- (4) Shishodia, S.; Sethi, G.; Aggarwal, B. B. *Ann. N.Y. Acad. Sci.* **2005**, *1056*, 206–217.
- (5) Niederau, C.; Gopfert, E. *MedKlin (Munich)* **1999**, *94*, 425–430.
- (6) Thakur, R.; Puri, H. S.; Husain, A. *Major medicinal plants of India*; Central Institute of Medicinal and Aromatic Plants: Lucknow, India, 1989.
- (7) Wilken, R.; Veena, M. S.; Wang, M. B.; Srivatsan, E. S. *Mol. Cancer* **2011**, *7*, 10–12.
- (8) Abe, Y.; Hashimoto, S.; Horie, T. *Pharmacol. Res.* **1999**, *39*, 41–47.
- (9) Aggarwal, B. B.; Sundaram, C.; Malani, N.; Ichikawa, H. *Adv. Exp. Med. Biol.* **2007**, *595*, 1–75.
- (10) Hatcher, H.; Planalp, R.; Cho, J.; Torti, F. M.; Torti, S. V. *Cell. Mol. Life Sci.* **2008**, *65*, 1631–1652.
- (11) Garg, R. K.; Kumari, H.; Kaur, R. *Egypt. J. Forensic Sci.* **2011**, *1*, 53–57.
- (12) Ferguson, L.; Bradshaw, R.; Wolstenholme, R.; Clench, M.; Francese, S. *Anal. Chem.* **2011**, *83*, 5585–5591.
- (13) Bisht, S.; Feldmann, G.; Soni, S.; Ravi, R.; Karikar, C.; Maitra, A.; Maitra, A. *J. Nanobiotechnol.* **2007**, *5*, 1–18.
- (14) Cooreya, R. V.; Håkansson, P. *Sri Lankan J. Phys.* **2003**, *4*, 11–20.
- (15) Maya, L. A.; Tourkina, E.; Hoffman, S. R.; Dix, T. A. *Anal. Biochem.* **2005**, *337*, 62–69.
- (16) Trim, P. J.; Djidja, M. C.; Atkinson, S. J.; Oakes, K.; Cole, L. M.; Anderson, D. M.; G., Hart, P. J.; Francese, S.; Clench, M. R. *Anal. Bioanal. Chem.* **2010**, *397*, 3409–3419.
- (17) Pabon, H. J. *Recueil Trav. Chimiques Pays-Bas* **1964**, *83*, 379–386.
- (18) Khan, M. A.; El-Khatib, R.; Rainsford, K. D.; Whitehouse, M. W. *Bioorg. Chem.* **2012**, *40*, 30–38.
- (19) Wolstenholme, R.; Bradshaw, R.; Clench, M. R.; Francese, S. *Rapid Commun. Mass Spectrom.* **2009**, *23*, 3031.
- (20) Puolitaival, S. M.; Burnum, K. E.; Cornett, D. S.; Caprioli, R. M. *J. Am. Soc. Mass Spectrom.* **2008**, *19*, 882–886.
- (21) Simmons, D. A. Improved MALDI-MS imaging performance using continuous laser rastering. In *ABI Technical Note*; MDS Analytical Technologies: Concord, Canada, 2008; accessed at [http://www.maldi-msi.org/download/TechNote\\_Raster\\_Imaging\\_QS.pdf](http://www.maldi-msi.org/download/TechNote_Raster_Imaging_QS.pdf).
- (22) Strohalm, M.; Kavan, D.; Novak, P.; Volny, M.; Havlicek, V. *Anal. Chem.* **2010**, *82*, 4648–4651.
- (23) Croxton, R. S.; Baron, M. G.; Butler, D.; Kent, T.; Sears, V. G. *Forensic Sci Int.* **2010**, *199*, 93–102.
- (24) Porta, T.; Grivet, C.; Kraemer, T.; Varesio, E.; Hopfgartner, G. *Anal. Chem.* **2011**, *83*, 4266–4272.
- (25) Earnshaw, C. J.; Carolan, V. A.; Richards, D. S.; Clench, M. R. *Rapid Commun. Mass Spectrom.* **2010**, *24*, 1665–1672.
- (26) Jovanovic, S. V.; Steenken, S.; Boone, C. W.; Simic, G. *J. Am. Chem. Soc.* **1999**, *121*, 9677–9681.
- (27) Sharma, R. A.; Gescher, A. J.; Steward, W. P. *Eur. J. Cancer* **2005**, *41*, 1955–1968.
- (28) Hart, P. J.; Francese, S.; Claude, E.; Woodroffe, M. N.; Clench, M. R. *Anal. Bioanal. Chem.* **2011**, *401*, 115–125.